Article ID: 1007-4627(2017) 01-0092-06

Medium-heavy Superdeformed Hypernuclei in Skyme Hartree-Fock Model

ZHOU Xianrong[1], E. Hiyama[2], H. Sagawa[2,3]

(*1. Department of Physics, East China Normal University, Shanghai 200241, China;*
2. Nishina Center for Accelerator-Based Science, Institute for Physical and Chemical Research, Wako 351-0198, Japan;
3. Center for Mathematics and Physics, Univeristy of Aizu, Aizu-Wakamatsu, Fukushsima 965-8560, Japan)

Abstract: The superdeformed (SD) states in medium heavy hypernuclei with core nuclei of Ar isotopes and ^{40}Ca are studied in the frame of Skyrme Hartree-Fock (SHF)+ BCS model together with a microscopic ΛN interaction. The calculation indicates that the Λ separation energy S_Λ of ground state is larger than that of SD state. The result is consistent with the antisymmetrized molecular dynamics (AMD) calculation, but inconsistent with that of relativistic mean field (RMF). The difference comes from the different interaction and density distribution in the core nuclei and the corresponding hypernuclei.

Key words: Skyrme Hartree-Fock model; superdeformation; hypernuclei
CLC number: O571.6 **Document code:** A **DOI:** 10.11804/NuclPhysRev.34.01.092

1 Introduction

One of the main purpose in hypernuclear physics is to study the effect of the additional hyperon(s) on the core nuclei. Due to the shrinkage effect of a hyperon, it was pointed out that the additional hyperon affects the nuclear shape. Recently, the effect of hyperon(s) on the deformation in *p*-shell and *sd*-shell hypernuclei was studied self-consistently in nonrelativistic Skyrme-Hartree-Fock (SHF) mean-field model[1–4], relativistic mean field (RMF)[5], and then antisymmetrized molecular dynamics(AMD)[6]. In general, the deformation of hypernuclei is a little bit smaller than that of the core nuclei due to the shrink effect of hyperon[1]. However, for the shape coexistent nuclei, the RMF predicts a drastic change of the deformation of the corresponding hypernuclei due to the additional hyperon, such as in $^{13}_{\Lambda}$C and $^{29}_{\Lambda}$Si[2, 5]. Therefore, the polarization effect of hyperons is larger in RMF model than that in nonrelativistic SHF model[3]. However, in an extended AMD calculations for $p-sd$ shell hypernuclei, it was found that Λ hyperon in the p wave enhances nuclear deformation, while that in the s wave reduces it[6]. Therefore, the effect of hyperons on nuclear shapes depends on different models.

In beyond *sd*−shell nuclei, there exist superdeformation (SD) states. What happens when injecting a hyperon into SD nuclei? To study the effect of hyperon on SD nuclei, it is better to choose light SD nuclei. Recently, in $A\sim40$ nuclei, the SD bands have been observed in the even-even ^{36}Ar[7] and ^{40}Ca[8] nuclei and also recently in odd-A nucleus ^{35}Cl[9]. In Ref. [10], it was predicted, for the first time, that the SD states exist in the hypernuclei $^{41}_{\Lambda}$Ca and $^{46}_{\Lambda}$Sc. It was also found that the Λ separation energy B_Λ becomes smaller as the quadrupole deformation increases. The Λ separation energy is smaller in SD state than that in normal deformed state or spherical state according to the calculation in $^{46}_{\Lambda}$Sc and $^{48}_{\Lambda}$Sc with AMD[10]. However, the conclusion is opposite to the RMF calculation of SD states and the corresponding hypernuclei of Ar isotopes[11]. It was found that the Λ separation energy B_Λ in the SD state is larger than that of a normally deformed or spherical ground state. The reason of the difference is because in RMF, the density profiles of SD states in Ar isotopes have a strong localization with a ring structure near the surface and the central part of the density is dilute, showing a hole structure. The localization of SD density results in an appreciable deformation in the hyperon wave function and then a large overlap between the core and the hyperon in the SD hypernuclei of Ar isotopes. In this sense, there is a strong model dependence on the structure of SD hypernuclei. It will be quite interesting and important

Received date: 15 Sep. 2016
Foundation item: National Natural Science Foundation of China (11275160)
Biography: ZHOU Xianrong(1974–), female, Hefei, Anhui, Professor, working on nuclear structure;
E-mail: xrzhou@phy.ecnu.edu.cn.

to apply a well-established mean field Skyrme model to study SD hypernuclei to see how SHF model[12] justifies the previous results of RMF or AMD and what is the difference among the three models.

2 Extended skyrme energy density functionals including hyperon-nucleon interaction

In the present extended SHF model[1] for hypernuclei, the hyperon-nucleon interaction NSC89[3] is added to the nucleon sector a modern Skyrme energy density function SkI4[13]. The total energy of a hypernucleus in the extended SHF model is written as

$$E=\int \mathrm{d}^3\boldsymbol{r}\,\epsilon_{\mathrm{ESHF}}(\boldsymbol{r}) \tag{1}$$

with the energy density functional

$$\epsilon_{\mathrm{ESHF}}=\epsilon_{\mathrm{N}}[\rho_{\mathrm{n}},\rho_{\mathrm{p}},\tau_{\mathrm{n}},\tau_{\mathrm{p}},\boldsymbol{J}_{\mathrm{n}},\boldsymbol{J}_{\mathrm{p}}]+\epsilon_{\Lambda}[\rho_{\mathrm{n}},\rho_{\mathrm{p}},\rho_{\Lambda},\tau_{\Lambda}] \tag{2}$$

where ϵ_{N} is the total energy density of nucleons[14, 15], and ϵ_{Λ} is the hyperon-nucleon energy density functional. The local density ρ_{q}, kinetic density τ_{q}, and spin-orbit current $\boldsymbol{J}_{\mathrm{q}}$ read

$$\rho_{\mathrm{q}}=\sum_{k\in\Omega_{\mathrm{q}}} v_k^2|\phi_k^{\mathrm{q}}|^2\ , \tag{3}$$

$$\tau_{\mathrm{q}}=\sum_{k\in\Omega_{\mathrm{q}}} v_k^2|\nabla\phi_k^{\mathrm{q}}|^2\ , \tag{4}$$

$$\boldsymbol{J}_{\mathrm{q}}=-\frac{i}{2}\sum_{k\in\Omega_{\mathrm{q}}} v_k^2\left[\phi_k^{\mathrm{q}\dagger}\nabla\times\hat{\sigma}\phi_k^{\mathrm{q}}-\phi_k^{\mathrm{q}\dagger}(\nabla\times\hat{\sigma})^{\dagger}\phi_k^{\mathrm{q}}\right] \tag{5}$$

where ϕ_k are the single-particle wave functions of the Ω_{q} occupied states for the particles of kind $q=\mathrm{n},\mathrm{p},\Lambda$, respectively. And v_k^2 are the occupation probabilities (for nucleons only) calculated by BCS approximation by taking a residual pairing interaction into account. In the calculation, the density-dependent delta force is adopted in the pairing channel[16],

$$V(\boldsymbol{r}_1,\boldsymbol{r}_2)=V_0\left(1-\frac{\rho(\boldsymbol{r})}{\rho_0}\right)\delta(\boldsymbol{r}_1-\boldsymbol{r}_2)\ , \tag{6}$$

where $\rho(\boldsymbol{r})$ is the HF density at $\boldsymbol{r}=(\boldsymbol{r}_1+\boldsymbol{r}_2)/2$ and $\rho_0=0.16\ \mathrm{fm}^{-3}$. The pairing strength is taken to be $V_0=-410$ MeV fm^3 for both neutrons and protons[17].

The energy density functional of hyperon-nucleon ϵ_{Λ} is written as in Ref. [18],

$$\epsilon_{\Lambda}=\frac{\tau_{\Lambda}}{2m_{\Lambda}}+\epsilon_{\mathrm{N}\Lambda}(\rho_{\mathrm{n}},\rho_{\mathrm{p}},\rho_{\Lambda})+\left(\frac{m_{\Lambda}}{m_{\Lambda}^*(\rho_{\mathrm{n}},\rho_{\mathrm{p}},\rho_{\Lambda})}-1\right)\left(\frac{\tau_{\Lambda}}{2m_{\Lambda}}-\frac{3}{5}\frac{C}{2m_{\Lambda}}\rho_{\Lambda}^{5/3}\right)\ , \tag{7}$$

with $C=(3\pi^2)^{2/3}\approx 9.571$ and

$$\epsilon_{\mathrm{N}\Lambda}=(\rho_{\mathrm{n}}+\rho_{\mathrm{p}}+\rho_{\Lambda})B(\rho_{\mathrm{n}},\rho_{\mathrm{p}},\rho_{\Lambda})/A-(\rho_{\mathrm{n}}+\rho_{\mathrm{p}})B(\rho_{\mathrm{n}},\rho_{\mathrm{p}},0)/A-\frac{3}{5}\frac{C}{2m_{\Lambda}}\rho_{\Lambda}^{5/3}\ , \tag{8}$$

obtained from a fit to the binding energy per baryon, $B(\rho_{\mathrm{n}},\rho_{\mathrm{p}},\rho_{\Lambda})/A$, of asymmetric hypermatter, as generated by BHF calculations[19]. The adequate Λ effective mass,

$$\frac{m_{\Lambda}^*}{m_{\Lambda}}=\left[1+\frac{U_{\Lambda}(k_{\mathrm{F}}^{(\Lambda)})-U_{\Lambda}(0)}{{k_{\mathrm{F}}^{(\Lambda)}}^2/2m}\right]^{-1}\ , \tag{9}$$

is computed from the BHF single-particle potentials $U_{\Lambda}(k)$ obtained in the same calculations. In practice we use the parametrizations of hyperon-nucleon energy density and Λ effective mass in terms of the proton, neuron and hyperon densities $\rho_{\mathrm{n}},\rho_{\mathrm{p}},\rho_{\Lambda}$ as is given in references[1, 19].

Minimizing the total energy Eq. (1) with respect to nuclear density (hyperon density) one gets the Schrödinger equation for nucleons (hyperon),

$$\left[-\nabla\cdot\frac{1}{2m_{\mathrm{q}}^*(\boldsymbol{r})}\nabla+V_{\mathrm{q}}(\boldsymbol{r})-\mathrm{i}\nabla W_{\mathrm{q}}(\boldsymbol{r})\cdot(\nabla\times\boldsymbol{\sigma})\right]\phi_i^{\mathrm{q}}(\boldsymbol{r})=e_i^{\mathrm{q}}\phi_i^{\mathrm{q}}(\boldsymbol{r})\ , \tag{10}$$

where the modified HF potential by hyperon for nucleons is given by,

$$V_{\mathrm{q}}=V_{\mathrm{q}}^{\mathrm{SHF}}+\frac{\partial\epsilon_{N\Lambda}}{\partial\rho_{\mathrm{q}}}+\frac{\partial}{\partial\rho_{\mathrm{q}}}\left(\frac{m_{\Lambda}}{m_{\Lambda}^*}\right)\left(\frac{\tau_{\Lambda}}{2m_{\Lambda}}-\frac{3}{5}\frac{C}{2m_{\Lambda}}\rho_{\Lambda}^{5/3}\right)\ . \tag{11}$$

Here, $V_{\mathrm{q}}^{\mathrm{SHF}}$ (q =n,p) is the nucleonic Skyrme mean field potential without hyperons and W_{N} is the nucleonic spin-orbit potential as given in Refs. [14, 15]. The nucleon mean field is thus modified due to the presence of hyperons, causing a rearrangement of the nucleonic structure of a hypernucleus. The hyperon potential in Eq. (10) reads

$$V_{\Lambda}=\frac{\partial\epsilon_{\mathrm{N}\Lambda}}{\partial\rho_{\Lambda}}+\frac{\partial}{\partial\rho_{\Lambda}}\left(\frac{m_{\Lambda}}{m_{\Lambda}^*}\right)\left(\frac{\tau_{\Lambda}}{2m_{\Lambda}}-\frac{3}{5}\frac{C}{2m_{\Lambda}}\rho_{\Lambda}^{5/3}\right)-\left(\frac{m_{\Lambda}}{m_{\Lambda}^*}-1\right)\frac{C}{2m_{\Lambda}}\rho_{\Lambda}^{2/3}\ , \tag{12}$$

In the current calculation, axial symmetry is assumed for the SHF potentials and the Schrödinger equation is solved in cylindrical coordinates (r,z).

3 Results and discussion

In Fig. 1, we illustrate the energy surfaces of ^{40}Ca and Ar nuclear isotopes with $A = 36$, 38 and 40 and the corresponding Λ hypernuclei. The energy surfaces of hypernuclei are shifted 14 MeV upward for a displaying purpose. First let us discuss about Ca Isotope. As shown in Fig. 1(a), we have four minima in the energy surface. The ground state of core nucleus ^{40}Ca is spherical with $\beta_2 = 0$. The corresponding state of the Λ hypernucleus, $^{41}_{\Lambda}$Ca is also spherical. Three local energy minima in ^{40}Ca and $^{41}_{\Lambda}$Ca, are oblate and prolate normally deformed states with $\beta_2 \sim -0.3$, and 0.4, respectively, and a superdeformed state with $\beta_2 \sim 0.6$. In ^{36}Ar and ^{40}Ar and corresponding Λ hypernuclei, we have three energy minima. The ground states for these nuclei and the corresponding hypernuclei are oblate with $\beta_2 \sim -0.2$. We have also superdeformed energy minima for each nucleus and corresponding hypernucleus with $\beta_2 \sim 0.5$. On the other hand, in ^{38}Ar and $^{39}_{\Lambda}$Ar, we have only one shallow local minimum with $\beta_2 \sim 0$. The energy surface between $\beta_2 \sim 0.4$ and 0.6 is quite flat. Therefore, we do not find any clear sign of superdeformed state in this nucleus and its hypernucleus, which is different from the work in Refs. [11, 20].

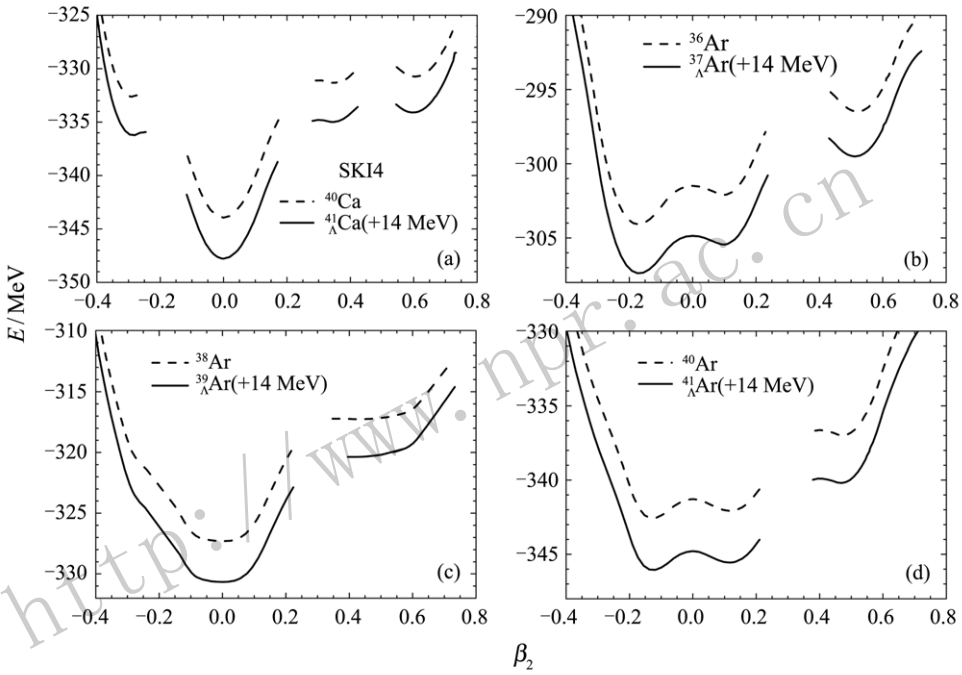

Fig. 1 (color online) The calculated energy surfaces of (a) ^{40}Ca and $^{41}_{\Lambda}$Ca (b) ^{36}Ar and $^{37}_{\Lambda}$Ar, (c) ^{37}Ar and $^{38}_{\Lambda}$Ar, and (d) ^{39}Ar and $^{40}_{\Lambda}$Ar as a function of the deformation parameter β_2. The Skyrme interaction SkI4 is used for nucleonic part, while the NSC89 potential is used for ΛN interaction. The energy surfaces of hypernuclei are shifted by 14 MeV upward for a displaying purpose.

In Table 1, we list the quadrupole deformation parameters, Λ separation energies S_Λ defined by

$$S_\Lambda = E(^{A+1}_{\Lambda}Z) - E(^{A}Z) \ , \tag{13}$$

and the overlap between the core and hyperon $I_{\rm overlap}$ defined by

$$I_{\rm overlap} = \int \rho_{\rm core}(r,z)\rho_\Lambda(r,z) r {\rm d}r{\rm d}z, \quad r = \sqrt{x^2+y^2} \ . \tag{14}$$

It is interesting to see the S_Λs in each hypernuclei. The calculated S_Λs in all Λ hypernuclei are smaller by about 1 MeV than those in Refs. [11, 20]. The reason why the present calculations are much smaller is the depth of single particle energy U_Λ. The U_Λ using present ΛN interaction, NSC89, is about 25 MeV, which is less attractive than the U_Λs with about 30 MeV depth in Ref. [11] in which ESC08 interaction was used. When a Λ particle is added to these nuclei, as shown in Table 1, S_Λs in superdeformed states of Ar isotopes and $^{41}_{\Lambda}$Ca are smaller than those of the ground states of the corresponding hypernuclei, which is inconsistent with the work in RMF[11], but consistent with the work by AMD calculation[10] although the present energy differences of S_Λ in each hypernuclei is smaller than those of AMD calculation. The authors in Ref. [11] mentioned the reasons why the S_Λs in superdeformed states in Ar and ^{40}Ca are much larger than those in the ground state. That is from the overlap between the density of core nucleus $\rho_{\rm core}$ and the density of hyperon ρ_Λ. In order to investigate

them, first as shown in Table 1, we discuss $I_{\rm overlap}$. In the RMF calculation of Ref. [11], the calculated $I_{\rm overlap}$s in all of superdeformed states in Ar isotopes are larger than those in the ground states because of the strong localization with a ring structure near the surface. However, in the present work, the $I_{\rm overlap}$s in the superdeformed states in ${}^{41}_{\Lambda}$Ca, ${}^{37}_{\Lambda}$Ar and ${}^{39}_{\Lambda}$Ar are smaller than those in the ground states since in the present calculation there is no strong localization. Therefore, there is a correlation between the overlap between the density distribution of the core nucleus and the hyperon $I_{\rm overlap}$ and Λ separation energy S_Λs in RMF and SHF. If there is a strong localization with a ring structure near nuclear surface, $I_{\rm overlap}$ of SD state will be larger than that of spherical or ND state and so is the S_Λ, and vice versa.

Table 1　The quadrupole deformation parameters, Λ separation energies (S_Λ) and spatial overlap between Λ and nucleons ($I_{\rm overlap}$) at the GS and SD (with asterisks) minima in ^{40}Ca, ^{36}Ar, ^{38}Ar, ^{40}Ar and the corresponding hypernuclei. Values of S_Λ and $I_{\rm overlap}$ calculated by RMF and AMD are listed in parentheses, respectively.

Nucleus	β_2	S_Λ	$I_{\rm overlap}$
${}^{41}_{\Lambda}$Ca	0.000	17.836 (18.553, 18.66)	0.131 6 (0.136 1, 0.136 4)
${}^{41}_{\Lambda}$Ca*	0.594	17.363 (19.242, 17.70)	0.129 9 (0.139 3, 0.133 6)
${}^{37}_{\Lambda}$Ar	−0.165	17.293 (18.177, 18.59)	0.129 9 (0.135 2, 0.133 8)
${}^{37}_{\Lambda}$Ar*	0.515	17.122 (18.524, 18.04)	0.128 4 (0.137 0, 0.131 0)
${}^{39}_{\Lambda}$Ar	0.000	17.379 (18.441, 18.55)	0.131 8 (0.136 0, 0.141 6)
${}^{41}_{\Lambda}$Ar	−0.118	17.478 (18.785, 19.27)	0.131 8 (0.135 7, 0.135 3)
${}^{41}_{\Lambda}$Ar*	0.455	17.171 (19.070, 18.99)	0.131 8 (0.137 8, 0.137 0)

The density profiles in ^{40}Ca, Ar isotopes, and the corresponding hypernuclei are plotted in Fig. 2. We see no localized density profiles in Fig. 2 despite of the fact seen in RMF calculation in Ref. [11]. This is similar to AMD calculation in Refs. [10, 20]. Therefore, it is reasonable that the S_Λs in SD state are smaller than those in the ground states. In comparison to the density distribution by AMD[10, 20], the present nucleon densities seem more dilute than those in AMD calculation. When a Λ particle is added into the core nuclei, the densities become dynamical contraction for each system from Fig. 2(a) to (c).

In Fig. 3, the calculated Λ−nucleon potentials of the ground state and the SD state in ${}^{37}_{\Lambda}$Ar with the SHF model are compared with those obtained by the

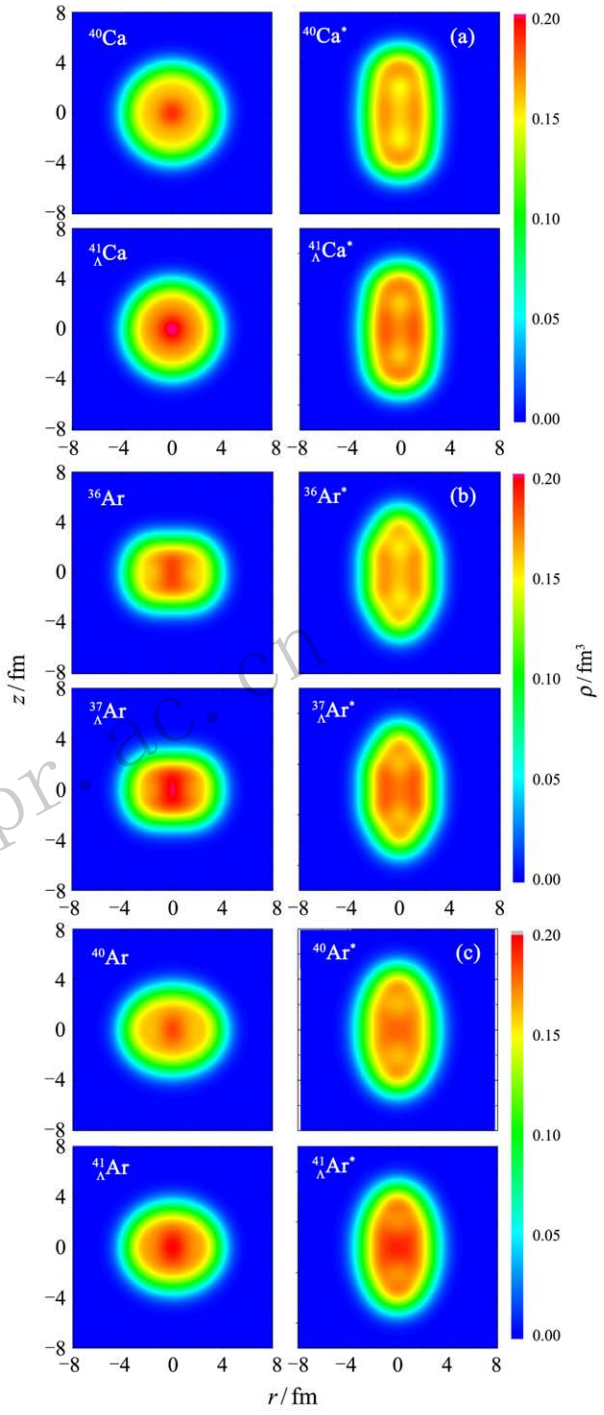

Fig. 2　(color online) Two-dimensional density distributions in the $r-z$ plane ($r=\sqrt{x^2+y^2}$ and z axis is the symmetric one) for (a)^{40}Ca and ${}^{41}_{\Lambda}$Ca, (b) ^{36}Ar and ${}^{37}_{\Lambda}$Ar, (c) ^{40}Ar and ${}^{41}_{\Lambda}$Ar, and (c). The asterisks denote SD states.

RMF model with an effective Lagrangian PK1-Y1. For both $r-$ and $z-$ direction, the mean field potentials of Λ hyperon of SHF are shallower than those of RMF model by $4\sim5$ MeV. This is the reason why the RMF model predicts a larger Λ separation energy S_Λ than that of SHF model.

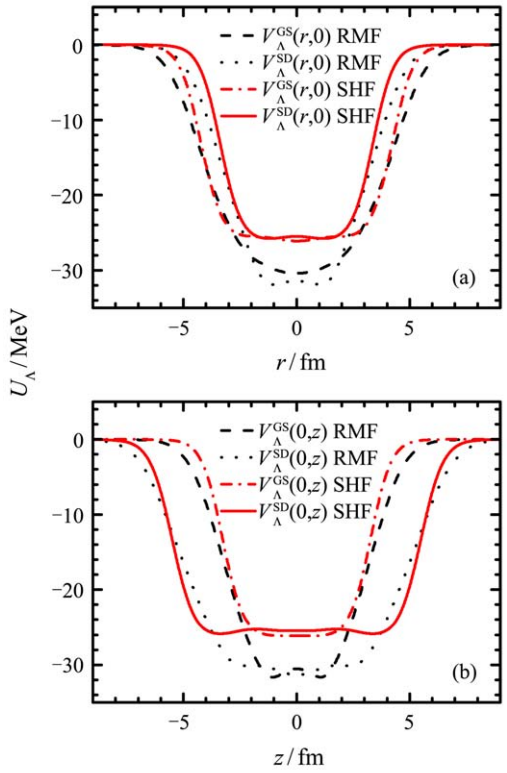

Fig. 3 (color online) The Λ−nucleon potentials of the ground state and the SD state in ${}^{37}_{\Lambda}$Ar. The SHF potentials are calculated by using a Skyrme interaction SkI4 with the hyperon-nucleon interaction NSC89, while the RMF potentials are calculated by using an effective Lagrangian PK1-Y1.

4 Summary

The SHF+BCS calculation for ^{40}Ca, ^{36,38,40}Ar and the corresponding hypernuclei indicates that the Λ separation energy S_Λ of ground state is larger than that of SD state. The results are consistent with the AMD calculation, but opposite to RMF calculations. The difference of S_Λ between the present and RMF calculation comes from the strong localization with a ring structure of the SD states in ^{36,38,40}Ar isotopes and ^{40}Ca in RMF, while in the SHF and AMD calculation, there is no localization of nucleons with a ring-shape. And the different density distribution is determined by the potential used in different models. In this sense, the SHF calculation is similar to that of AMD, but it does not agree with that of RMF. We also recognize that the separation energy S_Λ is very sensitive to the adopted ΛN interactions while they are determined by some microscopic models or phenomenological parametrizations such as the nuclear matter calculations or microscopic many-body models.

References:

[1] ZHOU X R, SCHULZE H J, SAGAWA H, *et al.* Phys Rev C, 2007, **76**: 034312.
[2] WIN M T, HAGINO K. Phys Rev C, 2008, **78**: 054311.
[3] SCHULZE H J, WIN M T, HAGINO K, *et al.* Prog Theor Phys, 2010, **123**: 569.
[4] WIN M T, HAGINO K, KOIKE T. Phys Rev C, 2011, **83**: 014301.
[5] LU B N, ZHAO E G, ZHOU S G. Phys Rev C, 2011, **84**: 014328.
[6] ISAKA M, KIMURA M, DOTE A ,*et al.* Phys Rev C, 2011, **83**: 044323.
[7] SVENSSON C E, MACCHIAVELLI A O, JUODAGALVIS A, *et al.* Phys Rev C, 2001, **63**: 061301(R).
[8] IDEGUCHI E, SARANTITES D G, REVIOL W, *et al.* Phys Rev Lett, 2001, **87**: 222501.
[9] BISOI A, SARKAR M S, SARKAR S, *et al.* Phys Rev C, 2013, **88**: 034303.
[10] ISAKA M, FUKUKAWA K, KIMURA M, *et al.* Phys Rev C, 2014, **89**: 024310.
[11] LU Bingman, HIYAMA E, SAGAWA H, *et al.* Phys Rev C, 2014, **89**: 044307.
[12] ZHOU X R, HIYAMA E, SAGAWA H. Phys Rev C, 2016, **94**: 024331.
[13] REINHARD P G, FLOCARD H. Nucl Phys A, 1995, **584**: 467.
[14] VAUTHERIN D. Phys Rev C, 1973, **7**: 296.
[15] BENDER M, RUTZ K, REINHARD P G. Phys Rev C, 1999, **60**: 034304.
[16] TAJIMA N, BONCHE P, FLOCARD H, *et al.* Nucl Phys A, 1993, **551**: 434.
[17] SAGAWA H, SUZUKI T, HAGINO K. Nucl Phys A, 2003, **722**: C183; Phys Rev C, 2003, **68**, 014317.
[18] CUGNON J, LEJEUNE A, SCHULZE H J. Phys Rev C, 2000, **62**: 064308; VIDAÑA I, POLLS A, RAMOS A, *et al.* Phys Rev C, 2001, **64**: 044301.
[19] SCHULZE H J, LEJEUNE A, CUGNON J, *et al.* Phys Lett B, 1995, **355**: 21; SCHULZE H J, BALDO M ,OMBARDO U L, *et al.* Phys Rev C, 1998, **57**: 704; Phys Rev C, 2000, **61**: 055801; SCHULZE H J, POLLS A, RAMOS A, *et al.* Phys Rev C, 2006, **73**: 058801.
[20] ISAKA M, KIMURA M, HIYAMA E, *et al.* Prog Theor Exp, 2015, **103**: 02.

Skyrme Hartree-Fock 模型对中等质量超形变超核的研究

周先荣[1,1)]，E. Hiyama[2]，H. Sagawa[2,3]

（1. 华东师范大学物理系，上海 200241；
2. 日本理化学研究所仁科加速器科学中心，和光 351-0198，日本；
3. 日本会津大学数理中心，会津 965-8560，日本）

摘要： 采用 Skyrme Hartree-Fock 模型和微观的核子-超子相互作用对 Ar 同位素和 ^{40}Ca 及相应超核的超形变态进行了研究，计算结果表明，基态的 Λ 超子分离能比激发态的大。这一结果与反对称化分子动力学模型的结果一致，而与相对论平均场的结果相反。这区别主要来源于不同模型中不同的相互作用导致的核心核及相应超核密度分布的不同。

关键词： Skyrme Hartree-Fock模型；超形变；超核

收稿日期： 2016-09-15

基金项目： 国家自然科学基金资助项目 (11275160)

1)　E-mail: xrzhou@phy.ecnu.edu.cn。